



# Reservoir operation under influence of the joint uncertainty of inflow and evaporation

Omid Bozorg-Haddad<sup>1</sup> · Pouria Yari<sup>1</sup> · Mohammad Delpasand<sup>2</sup> · Xuefeng Chu<sup>3</sup>

Received: 2 January 2020 / Accepted: 1 June 2021 / Published online: 15 June 2021  
© The Author(s), under exclusive licence to Springer Nature B.V. 2021

## Abstract

Reservoirs play a major role as an essential source of surface water, especially in arid and semi-arid regions. To optimize the operation of a reservoir and determine its storage, which varies in time, the uncertainties of major influencing factors such as its inflow and evaporation should be considered. The objective of this study is to examine the effects of joint uncertainties of the inflow and evaporation of Durudzan reservoir on its performance for the first time. The Monte Carlo simulation is used for uncertainty assessment. Specifically, the monthly time series of inflow and evaporation were generated by using artificial neural networks and the standard operation policy was used for reservoir operation. Furthermore, the probabilistic distributions of four performance indices, including time-based reliability, volumetric reliability, vulnerability, and resiliency were calculated to assess the effects of the joint uncertainties of inflow and evaporation as well as the physical parameters on the reservoir variables (e.g., water release, storage, and spill). The results showed that the highest and lowest uncertainties of the reservoir water release occurred in July and May, respectively. In addition, the highest and lowest uncertainties were, respectively, observed in March and October for the reservoir storage, and in March and May for the water spill. The results also showed that the volumetric reliability had the highest uncertainty with a coefficient of variation (CV) of 0.158, while the resiliency had the lowest uncertainty with a CV of 0.020.

**Keywords** Reservoir operation management · Artificial neural network (ANN) · Probability distribution · Uncertainty analysis · Monte Carlo simulation · Reservoir performance indices

## 1 Introduction

Increasing population and consequently increasing water demand for various needs require optimal water resources development and management (Bozorg-Haddad et al., 2009; Chang & Chang, 2009; Delli Priscoli, 2000; Delpasand et al., 2020; Shokri et al., 2013). In this regard, reservoirs, as one of the main sources of surface water, play an essential role in

---

✉ Omid Bozorg-Haddad  
OBHaddad@ut.ac.ir

Extended author information available on the last page of the article

meeting the water needs and reducing the potential damages caused by destructive floods, especially in arid and semi-arid regions (Akbari-Alashti et al., 2014; Asgari et al., 2016; Bozorg-Haddad et al., 2020; Liu et al., 2017). The water balance of a reservoir is affected by many factors such as its inflow, evaporation from the free surface, direct rainfall, water leakage and percolation, and water release, which are uncertain. Therefore, to develop a comprehensive and optimal operation policy for a reservoir system, the uncertainties of meteorological and hydrological processes/variables should be considered (Bozorg-Haddad et al., 2014, 2019). By knowing the volume of storage, it is possible to operate the reservoir and implement different utilization projects. Generally, simulation and optimization policies are used for reservoir operation (Loucks et al., 1981). Simulation methods have been a fundamental tool for planning and managing reservoirs. Reservoir simulation models are usually based on the mass balance equation, which shows the reservoir's hydrological behavior in response of its water inputs, outputs, and operating conditions (Bozorg-Haddad, 2018). In addition, uncertainty is a major factor that needs to be considered in water resources planning and management. Decision making in reservoir operation often involves the uncertainties of natural phenomena and inaccurate characterization of important parameters and variables. Thus, ignoring such uncertainties may lead to overestimation or underestimation of the performance of a reservoir in the development of its operation rules (Loucks & van Beek, 2005; Tehrani et al., 2008). Reservoir performance indices are usually used to evaluate the operation of the system. Important indices include reliability, vulnerability, and resiliency (Bozorg-Haddad et al., 2014; Srdjevic et al., 2004).

Lowe et al. (2009) evaluated the uncertainty of evaporation from water supply reservoirs by developing a framework for determining the uncertainties of the reservoir evaporation estimated by using the pan coefficient method. Their results showed that the largest decrease in uncertainty was gained by installing an evaporation pan at the reservoir. Zhang et al. (2009) evaluated four types of Bayesian neural network and applied for estimating the uncertainties of streamflow simulations in two watersheds in Georgia and Idaho. The results showed that by considering informative prior knowledge and using a variable model structure, the Bayesian neural networks provided more accurate quantification of the uncertainties of streamflow simulations. Zhao et al. (2011) proposed a method to explicitly quantify the uncertainty and assess the effect of the uncertainty of inflow on reservoir operation. Using a hypothetical example, they showed that the predicted uncertainty had a significant effect on the performance of the reservoir. Also, their results showed that the efficiency of reservoir operation decreased as the uncertainty increased, indicating that the efficiency was dependent on the forecast methods. By using two case studies from Norway and New Zealand, McMillan et al. (2017) emphasized the importance of streamflow uncertainty analysis in water management decisions and demonstrated that proper analysis and assessment of the uncertainties associated with streamflow data could effectively reduce the costs in water resources planning and management.

There is a need for long-term and short-term predictions of hydrologic processes in order to optimize a water resources system and/or plan for the future (Soltanjalili et al., 2011). In general, the artificial neural network (ANN) method has been widely used for such forecasting purposes and its effectiveness and performances have been demonstrated in many relevant applications (Cigizoglu, 2008). Bozorg-Haddad et al. (2016) used the ANN method to determine the optimal set of variables for streamflow forecasting and their results demonstrated the high accuracy of the ANN in runoff simulation. Application of the Monte Carlo simulation method for uncertainty analysis has gained significant attention (Soundharajan et al., 2016), because of its applicability in combining various forms of uncertainty (e.g., uncertainties associated with input data

and model) to estimate the final prediction uncertainty. Cremon et al. (2018) examined the convergence properties of the Monte Carlo simulation (MCS) of a reservoir model. They found that the use of a small ensemble (with a limit of 500 realizations) could yield errors of hundreds of percent. They concluded that it was possible to use large sets of realizations for profitability and decision-making analyses because of the parallel nature of MCS and also, optimization studies could benefit from using large ensembles, despite some difficulties. Tegegne and Kim (2020) considered the uncertainty of reservoir inflows by using the non-dominated sorting genetic algorithm II (NSGA-II) in their proposed reservoir operation rules and applied to the monthly operations of the Lake Tana multi-reservoir system in Ethiopia. Multiple performance measures demonstrated that their proposed model reached 84% of the perfect performance. Optimal operation of reservoirs needs multi-dimensional and integrated decision making, which involves many meteorological, hydrological, and socioeconomical variables such as rainfall, inflow, evaporation, and downstream water demands. Therefore, for future operation (e.g., water release) planning of reservoirs to meet different water demands and also effectively control floods, decision makers have to deal with various uncertainties associated with such variables (Seifollahi-Aghmiuni et al., 2016).

The uncertainties of evaporation and inflow of reservoirs have been evaluated in many studies. However, few efforts have been made to evaluate the uncertainties of water release and storage of reservoirs under the influence of joint uncertainties of the reservoir inflow and evaporation. The main objective of this study is to assess the uncertainties of the reservoir-related variables (e.g., water release and storage) by the Monte Carlo method, which is then applied to 47-year evaporation and inflow datasets of the Durudzan reservoir in Iran. Furthermore, by using the artificial neural network approach, probabilistic distribution functions are fitted for the evaporation and inflow data. Eventually, the uncertainties of water release and storage of the reservoir influenced by the uncertainties of its inflow and evaporation and different performance indices are evaluated. In this paper, the reservoir simulation model and Monte Carlo method are described in Sect. 2; the site information and the specifications of the Durudzan reservoir are presented in Sect. 3; the results of the evaluations are discussed in Sect. 4; and the conclusions are summarized in Sect. 5.

## 2 Methods

For the ultimate aim of this study to assess the effects of the joint uncertainty of reservoir inflow and evaporation on its operation, a set of methods are used, which are described as follows.

### 2.1 Reservoir operation policy

For the operation of a reservoir, it is necessary to know when and how the available water is released to meet the downstream water needs. Since the future inflows and the storage volumes are uncertain, the main goal is to determine the best release from the reservoir for a range of possible inflows and storage conditions. The water mass balance equation for a reservoir can be expressed as (Bozorg-Haddad, 2018; Delpasand et al., 2021; Xu & Singh, 1998):

$$S_{t+1} = S_t + \hat{Q}_t - Re_t - Sp_t - (\hat{E}v_t - P_t) \cdot \left( \frac{A_t + A_{t+1}}{2} \right) \tag{1}$$

in which  $t$ =time period;  $S_{t+1}$ =volume of reservoir storage at the beginning of period  $t+1$  ( $10^6 \text{ m}^3$  or million cubic meter (MCM));  $\hat{Q}_t$ =volume of the inflow of the reservoir during period  $t$  (variable with uncertainty) ( $10^6 \text{ m}^3$ );  $Re_t$ =volume of water release from the reservoir in period  $t$  (decision variable) ( $10^6 \text{ m}^3$ );  $Sp_t$ =volume of water spill from the reservoir during period  $t$  ( $10^6 \text{ m}^3$ );  $\hat{E}v_t$ =net evaporation from the reservoir during period  $t$  (variable with uncertainty) (m);  $P_t$ =precipitation on the reservoir during period  $t$  (m); and  $A_t$ =water surface area of the reservoir at the beginning of period  $t$  ( $\text{km}^2$ ).

The standard operating policies (SOP) are used to operate the reservoir. According to the SOP, for example, if the volume of usable reservoir storage ( $S_t + \hat{Q}_t - Loss_t - S_{\min}$ ) in any time period (e.g., month) is greater than or equal to the volume of total water demand, the amount of water released from the reservoir is equal to the total water demand. Otherwise, only the usable water will be released. As shown in Eqs. (2) and (3), if the storage volume of the reservoir in period  $t$  is greater than the minimum operating volume of the reservoir, water release will be performed. If the storage of the reservoir in period  $t$  is less than the required minimum volume, no water will be released (Xu et al., 1998; Bozorg-Haddad et al., 2020).

$$Re_t \neq 0 \quad S_t + \hat{Q}_t - Loss_t - S_{\min} > 0 \tag{2}$$

$$S_t + \hat{Q}_t - Loss_t - S_{\min} < 0 \quad Re_t = 0 \tag{3}$$

In which  $S_{\min}$ =minimum operating reservoir volume ( $10^6 \text{ m}^3$ ); and  $Loss_t$ =net loss in period  $t$  ( $10^6 \text{ m}^3$ ) as defined below (Bozorg-Haddad et al., 2019; Xu & Singh, 1998):

$$Loss_t = (\hat{E}v_t - P_t) \cdot \left( \frac{A_t + A_{t+1}}{2} \right) \tag{4}$$

For the condition of Eq. (2), the water release can be controlled based on the water demand as follows (Fallah-Mehdipour et al., 2015):

$$S_t + \hat{Q}_t - Loss_t - S_{\min} \geq De_t \quad Re_t = De_t \tag{5}$$

$$S_t + \hat{Q}_t - Loss_t - S_{\min} < De_t \quad Re_t = S_t + \hat{Q}_t - Loss_t - S_{\min} \tag{6}$$

In which  $De_t$ =total volume of downstream water demand in period  $t$  ( $10^6 \text{ m}^3$ ).

If the reservoir storage exceeds the maximum operating storage, the excess water spills out of the reservoir. Otherwise, no water spill occurs, as expressed in Eqs. (7) and (8) (Fallah-Mehdipour et al., 2015).

$$S_t + \hat{Q}_t - Loss_t - Re_t > S_{\max} \quad Sp_t = S_t + \hat{Q}_t - Loss_t - Re_t - S_{\max} \tag{7}$$

$$S_t + \hat{Q}_t - Loss_t - Re_t \leq S_{\max} \quad Sp_t = 0 \tag{8}$$

in which  $S_{\max}$ =maximum operating storage of the reservoir ( $10^6 \text{ m}^3$ ).

### 2.2 Artificial neural networks

ANNs are based on the structure of the biological neural networks for various issues such as pattern recognition, clustering classification, and regression. The ability of neural networks to map a set of data with negligible error rates makes them a powerful tool for modeling natural processes. An artificial neural network follows the same biological process as the neuron as a single unit that plays two roles: (1) combining inputs in (X) and (2) combining these inputs with a specific threshold value ( $\theta$ ) to calculate the appropriate output (Araghinejad, 2013; Bozorg-Haddad et al., 2018; Okon et al., 2020). This process is shown in Fig. 1.

Mathematically, a neuron alone is not enough to solve practical problems. Therefore, a network of perceptron is used in parallel and series, called the neural network. The multi-layered perceptron or feedforward network is the most prominent type of artificial neural network. In the feedforward network, each node (neuron) is only allowed to connect to another node in the next layer, forcing it forward. These networks are summarized in sequence numbers, each of which shows the number of nodes in each layer. The layers

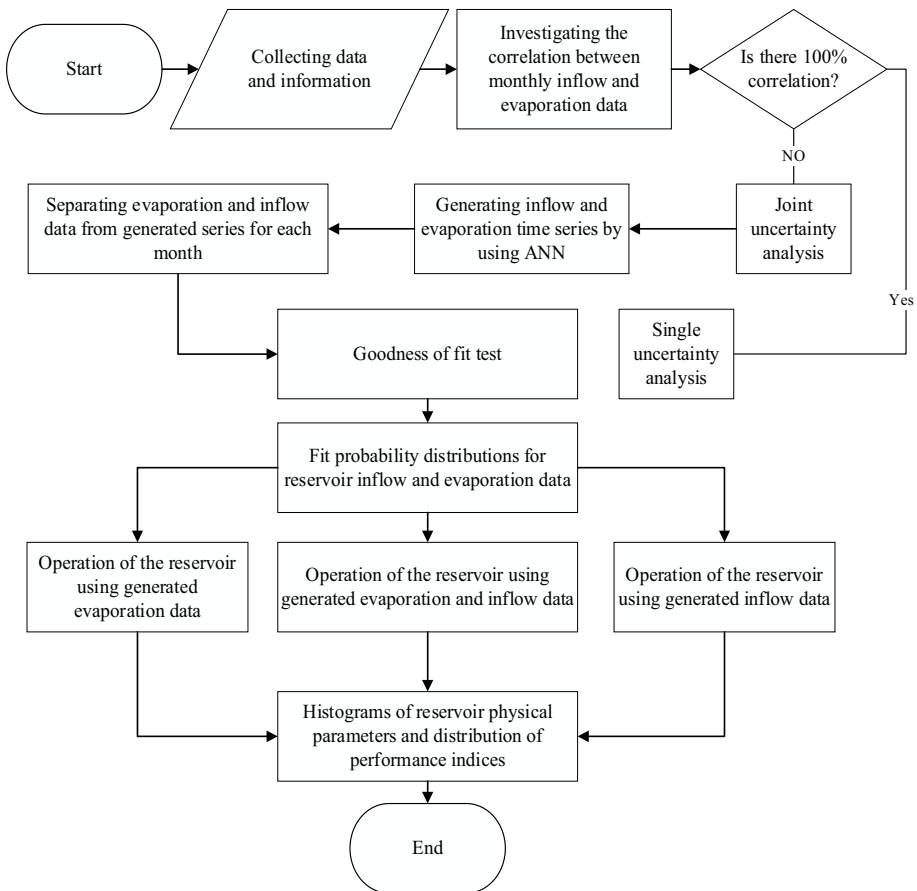


Fig. 1 Methodology flowchart

between the input and output are called hidden layers (Bozorg-Haddad et al., 2016; Ehsani et al., 2015; Fallah-Mehdipour et al., 2015; Jain et al., 1999).

For training the algorithm, the weights and biases of a neural network must be determined prior to the use of the network. Training is a phrase that usually refers to a supervised approach for determining weights and biases. One of the most commonly used methods for training in neural networks is the error propagation algorithm. To ensure high training accuracy and also prevent overfitting, a criterion is needed to stop the training process (e.g., control the number of repetitions (epoch)). After the training process, the network is ready to simulate the outputs associated with particular input vectors by using the resulting weights and biases.

In this study, a three-layer perceptron network with four neurons in the hidden layer was used. The Levenberg–Marquardt algorithm (Du & Stephanus, 2018; Iyer & Rhinehart, 1999) was used for network training. In the production process of the evaporation and inflow time series using the neural network, the 47-year evaporation and inflow data with time lags of one to six months, as well as 12, 24, 36 and 48 months were used as inputs and the time series of evaporation and inflow were produced as outputs. Note that the largest time lag was 48 months and the input and output data of the network were equal. So, 100 43-year time series were produced. The number of the inputs for the training process was 20 (10 pairs of the evaporation and inflow data) and the number of the outputs was two, which was the same as the generated evaporation and inflow. It should be noted that 70%, 15%, and 15% of the data were used for the training process, the validation process, and the test, respectively.

### 2.3 Goodness-of-fit test

The goodness-of-fit test is used to check how well sample data fit a particular statistical distribution from a population. The following steps are generally performed for such a test (González-Manteiga & Crujeiras, 2013):

- (1) Specify the Null hypothesis ( $H_0$ ) (Assume that the time series follows a particular statistical distribution)
- (2) Select the test method and statistic
- (3) Select the acceptance error and the level of trust for decision making
- (4) Calculate the test statistic for the sample data
- (5) Compare the series and make decisions based on the analysis

The Chi-square goodness-of-fit test was implemented in this study (Rolke & Gongora, 2020). This test was used to compare the theoretical distribution of the actual data. The test statistic is given by (Karamouz & Araghinejad, 2011):

$$\chi^2 = \sum_{i=1}^{NC} \frac{(f_i - \hat{f}_i)^2}{\hat{f}_i} \quad (9)$$

in which  $f$  = frequency of actual data;  $\hat{f}$  = expected frequency based on the theoretical distribution tested;  $i$  = data point number; and  $NC$  = total number of data points.

According to this test, at least 5 samples are recommended for each category (Karamouz & Araghinejad, 2011). The Chi-square distribution has  $(NC-NP-1)$  degrees of freedom, in which  $NP$  is the number of the estimated parameters for the desired

theoretical distribution. If the value calculated from Eq. (9) is less than the value of the Chi-square distribution (table values with the degree of freedom), the assumption of the admissibility of the information is accepted for the assumed distribution at a given acceptance level. In this study, after evaluating various distributions, the lognormal and normal distributions were, respectively, selected for the inflow and evaporation datasets because of their better performances.

## 2.4 Uncertainty analysis

No events or phenomena can be precisely predicted. The term of risk is used to describe the probability of failure. In order to increase the reliability of water supply from reservoir systems, various types of uncertainty associated with the variables should be considered in the design and operation of these systems. The main purpose of uncertainty analysis is to determine the statistical characteristics of the output of a model as a function of probability of input parameters (Lee et al., 2018). An uncertainty analysis provides a framework for identifying the uncertainty associated with the output of a model. In addition, uncertainty analysis specifies the designers' insight into the contribution of each of the probabilistic input parameters to the overall uncertainty of the model output. This knowledge is essential for identifying, evaluating, and analyzing the uncertainty of important parameters that require more attention in the analysis, design, and operation of water resources systems (Duckstein and Plate, 1987). Also, it should be noted that an additional source of uncertainty is associated with the model. This occurs as a result of unknown boundary conditions, simplifying assumptions, and the unknown effects and interactions of other variables that are not included. These uncertainties can be evaluated by comparing the results with other refined methods (Bai & Jin, 2016).

MCS was used for uncertainty assessment in this study. The model with random inputs generated random outputs. After many simulations, the probabilistic distributions of the output variables were determined. These distributions were used to estimate the reliability and other statistical properties (such as dispersion and skewness) of the distributions of the output variables. The MCS facilitated such multiple simulations to examine the system behaviors based on the changes in inputs (Maity, 2018). In this method, after identifying the indeterminate variables in the system's performance, a probabilistic distribution was considered for each variable and a series of random numbers were generated and used for simulations.

In this research, the MCS method was used to evaluate the impacts of evaporation and inflow of the reservoir on its performance. For this purpose, 100 time series of 47-year reservoir inflow data and the corresponding evaporation values were produced. Then, the statistics were generated for the reservoir operation. After operating the reservoir, its physical parameters and performance indices were extracted. To determine the effect of evaporation uncertainty on the output variables of the system, their probabilistic distributions were analyzed. Specifically, the evaporation uncertainty of each time series was evaluated based on the corresponding historical discharge data (i.e., inflow of the reservoir). Similarly, given the historical evaporation data, the effect of inflow uncertainty was assessed. In addition, the evaporation and inflow data were also used to investigate their joint uncertainty and the effects.

### 2.5 Performance indices for the reservoir system

Typically, the efficiency of a reservoir system is used to evaluate the performance of the model. The most important and useful criteria include reliability, resiliency, and vulnerability (; Delpasand et al., 2021).

The reliability of a reservoir system is quantified by the number of data in a satisfactory state divided by the total number of the data in the time series, indicating the likelihood that the reservoir is able to meet the downstream water demand.

(A). The time-based reliability can be expressed as (Hashimoto et al., 1982):

$$RT = \frac{N_w}{N} \tag{10}$$

in which  $RT$ =time-based reliability;  $N_w$ =number of satisfactory periods; and  $N$ =total periods.

(B). Similarly, the volumetric reliability can be written as (Ashofteh et al., 2019):

$$RV = \frac{\sum_{t=1}^T Re_t}{\sum_{t=1}^T De_t} \tag{11}$$

in which  $RV$ =volumetric reliability;  $\sum_{t=1}^T Re_t$ =total released water throughout the entire period; and  $\sum_{t=1}^T De_t$ =total water demand in the entire period.

It should be noted that the reliability criterion alone cannot determine the superiority of one system because this criterion does not specify the severity of the failure and the rate of return to success after each failure. Thus, the following criteria must also be defined.

The resiliency of a reservoir system represents its ability to recover from a failure state (unsatisfactory condition) and return to a satisfactory condition. The resiliency index can be expressed as (Bozorg-Haddad, 2018):

$$\varphi = \frac{f_r}{f_t} \tag{12}$$

in which  $\varphi$ =resiliency;  $f_r$ =number of the states, in which a reservoir is unsatisfactory (failure), but its next state is satisfactory; and  $f_t$ =total number of failures occurring during the entire operation period.

According to the definition, resiliency is equal to the probability of a success period after a failure period. It should be noted that during the reservoir operation period, if the system fails at all time steps or no failure occurs, the resiliency is not defined.

In the operation of water resource systems, the failure of a system usually does not have the same level of importance and impact. Vulnerability refers to the extent of possible system failures and can be expressed as (Hashimoto et al., 1982):

$$M_f = \text{Max}_{OP} \frac{(De_t - Re_t)}{De_t} \tag{13}$$

in which,  $M_f$ =largest failure observed in a continuous series of failures and  $OP$  = operation period. Equation 13 indicates that  $\frac{(De_t - Re_t)}{De_t}$  should be calculated for each failure period



$t$ , which is defined as lack of supply. The maximum lack of supply over the entire operation period is defined as the system vulnerability.

The methodology details of this study are shown in Fig. 1. The main aim of this study is to evaluate the effect of the joint uncertainties of evaporation and inflow of a reservoir on its release and storage. As shown in Fig. 1, for this purpose, after collecting the historical inflow and evaporation data, the correlation between these two variables is analyzed to assess their joint uncertainty possibility (refer to Jothivenkatachalam et al. (2010) for more information about correlation evaluation). If there is a 100% correlation between the two variables, the uncertainty assessment for one variable can be performed by assessing the uncertainty of the other variable. But if the correlation between the two variables is lower than 100%, their joint uncertainty should be assessed. The lower correlation, the lower accuracy of the single uncertainty analysis. Then, the ANN and Chi-square methods are, respectively, used for generating the related time series and performing the goodness-of-fit test. Probability distributions are then fitted on the evaporation and inflow data, individually and jointly. For the purpose of uncertainty assessment, the Monte Carlo simulation is implemented. The histograms of the physical parameters of the reservoir and the distributions of the performance indices are created.

### 3 Case study

The Kor River is the largest one in Southern Iran. The river basin is located in the northwest of Fars Province with geographical coordinates of [41°51':26°52' E] and [8°30':48°30' N] (Fig. 2). The drinking, agriculture, and industry sectors have priorities of water supply for the downstream water demands. Due to the droughts in recent years, the annual inflow of the reservoir and its water release for meeting the agricultural demand have been reduced, which caused extensive socioeconomic damages to the area. Also, the evaporation has increased due to the climatic impacts (e.g., temperature). Thus, it is necessary to assess the uncertainty of inflow and evaporation and improve the prediction of the reservoir storage. So, the ultimate goal of this study is to estimate the probability distribution of the reservoir output influenced by the uncertainties of inflow and evaporation to meet the water demands of the region, which would further help identify proper operation policies of the Durudzan reservoir. Table 1 shows the characteristics of the reservoir. It should be mentioned that the data of the Durudzan reservoir (such as the water demand and its inflow) were obtained from the Iran's Ministry of Energy.

As aforementioned, statistical analyses of the monthly reservoir inflow and evaporation time series over a 47-year period from 1964 to 2011 were performed. A water year used in the analyses ranged from October 1 to September 30. Figure 3 shows the maximum, mean, and minimum values of the reservoir inflow and evaporation in different months from October to September for the entire 47-year period. As shown in Fig. 3, there are a wide range of changes in the inflow and evaporation of the reservoir in the study period, implying that the uncertainties of these variables are inevitable. For uncertainty assessment, Monte Carlo simulation was used in this study. Note that this method has been widely used for this purpose in many studies (e.g., King & Simonovic, 2020; Marton & Paseka, 2017; Willis et al., 1984).

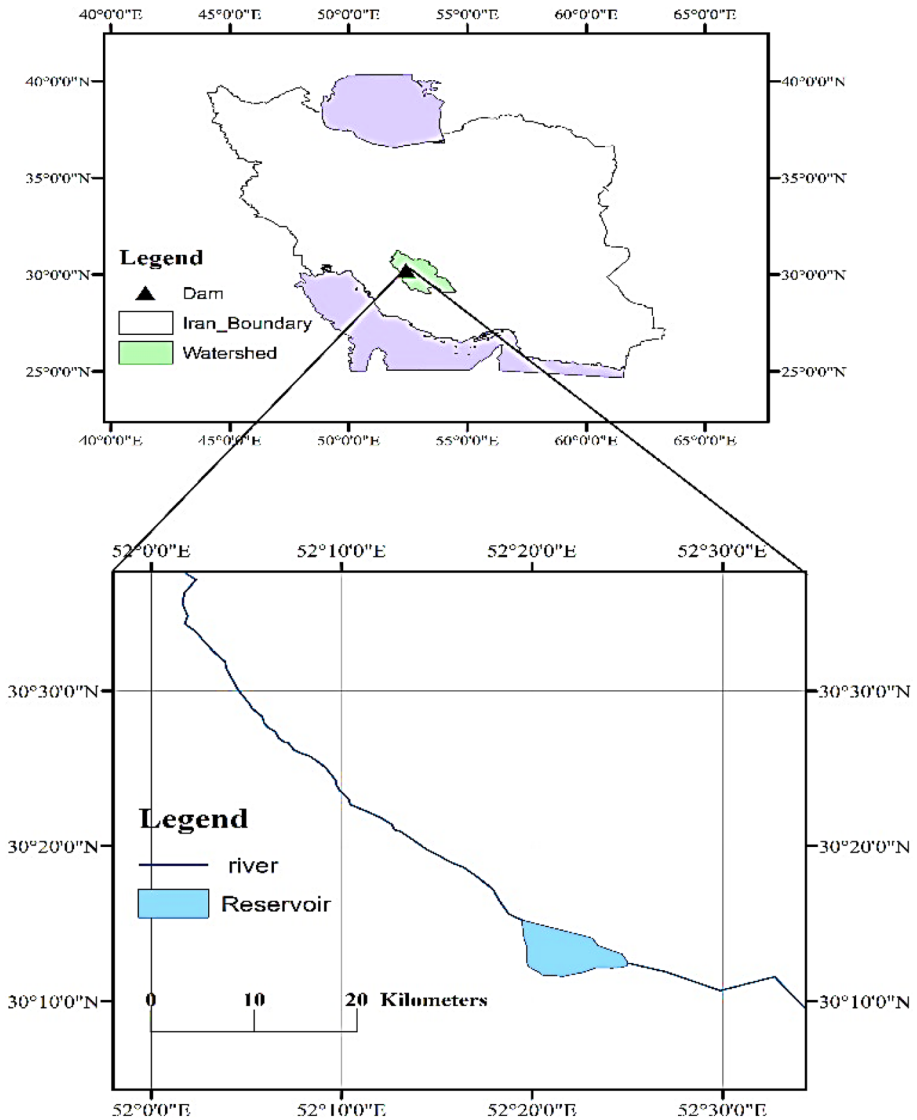


Fig. 2 Location of Durudzan dam in Southern Iran

## 4 Results and discussion

This study focused on assessing the influences of the joint uncertainty of evaporation and inflow on the release and storage of the Durudzan reservoir. For this purpose, the correlation between evaporation and inflow was first analyzed. Under the circumstance of lacking an acceptable correlation, the joint uncertainty assessment was performed. The results of this assessment are detailed below.

**Table 1** Physical characteristics of Durudzan reservoir

Physical characteristics	Values
Normal water elevation (meters above sea level)	1676.5
Storage at the normal water elevation ( $10^6 \text{ m}^3$ )	960.85
Dead storage ( $10^6 \text{ m}^3$ )	170
Equivalent water elevation to the dead storage (meters above sea level)	1650
Minimum experienced water elevation during operation (meters above sea level)	1658.77
Equivalent storage at the minimum experienced water elevation ( $10^6 \text{ m}^3$ )	275.48

#### 4.1 Neural network training for data generation

To determine the uncertainties of the evaporation and inflow of the reservoir, synthetic time series of these two variables were produced by using an artificial neural network. It should be noted that 70%, 15%, and 15% of the data were used for the training process, the validation process, and the test, respectively. Figure 4 shows the output values generated by the neural network versus the target values, as well as the correlation coefficient values for the training, validation, and test. It can be observed from Table 2 that October and March, respectively, had the lowest and highest inflows. April showed the highest standard deviation and the largest dispersion, whereas September had the least dispersion. Also, the values of the coefficient of variation obtained for the monthly historical and generated data showed that the dispersion of the generated data was lower than that of the historical data. It should be noted that when the inflow of the reservoir decreased, the evaporation was expected to increase since there was an inverse weak correlation between evaporation and discharge (or reservoir inflow), which varied from -0.60 to -0.045.

#### 4.2 Probability distribution of reservoir inflow

The Chi-square fitting test was used to measure the goodness of fit of the generated inflow data. The lognormal distribution was considered for the reservoir inflow data. Table 3 shows the results of the Chi-square test for the inflow data of all months. Since the inflows for all months obtained from the Chi-square test are smaller than the corresponding table values with the degree of freedom, it can be concluded that the desired assumption is valid, which confirms the probability distribution of the inflow data. Figure 5 shows the histograms of the generated inflow data for all months and their fitted lognormal distributions. As shown in Fig. 5, the largest dispersion occurred in April, while September had the smallest dispersion with a sharper peak.

#### 4.3 Probability distribution of reservoir evaporation

Table 3 shows the results of the Chi-square test for the evaporation data of all months. For all months, the evaporation values obtained from the Chi-square test are smaller

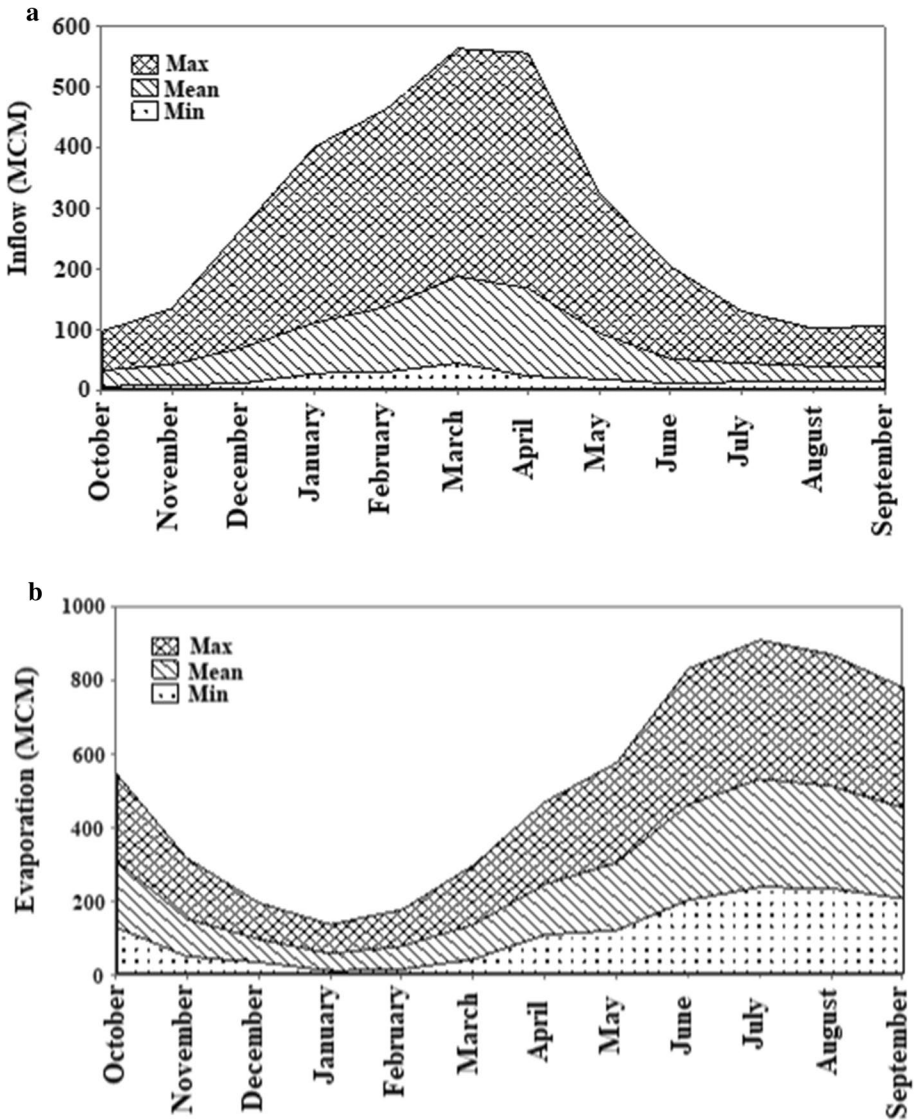


Fig. 3 Maximum, mean, and minimum values in different months **a** inflow **b** evaporation

than the corresponding table values with the degree of freedom. Thus, the assumption of the normal distribution of the evaporation data is accepted. Figure 6 shows the histograms of the evaporation data generated for all months, and their fitted normal distributions.

The evaporation histograms in Fig. 6 indicate that July and January, respectively, had the highest and lowest mean evaporation values. The highest and lowest standard deviation values of the generated and historical data occurred in July and December, respectively. The dispersion of the evaporation data was higher in the months with higher evaporation,

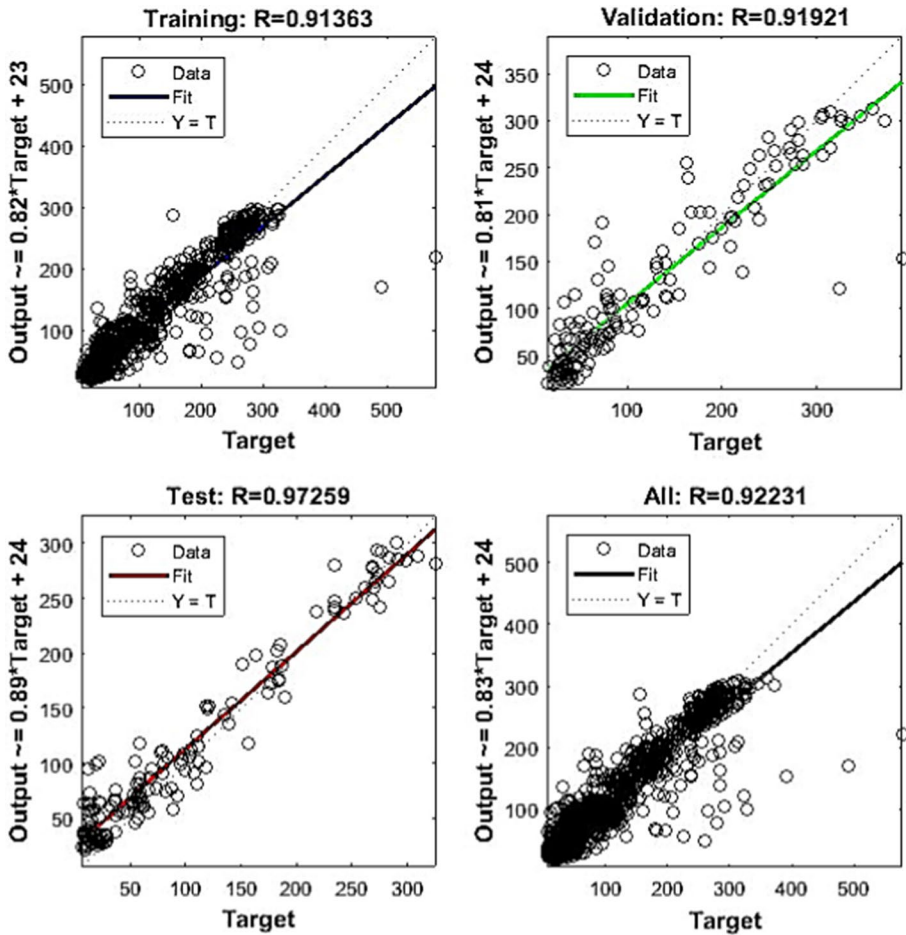


Fig. 4 Simulated vs. target values for the training, validation, test, and total datasets

and vice versa. Accordingly, the minimum dispersion of the evaporation data distribution was related to the months of December and January, while the distribution of the evaporation data in the months of July and August showed the largest dispersion.

#### 4.4 Effects of the uncertainties of evaporation and inflow on reservoir performance

To evaluate the effects of the uncertainties of evaporation and inflow on the reservoir performance, three reservoir performance indices (i.e., reliability, resiliency, and vulnerability) were used and the results are summarized as follows:

##### (1) Effect of evaporation uncertainty on reservoir release

Table 4 shows the results of the effect of the evaporation uncertainty on the reservoir release in April–October. According to Table 4, the highest uncertainty of water

**Table 2** Mean, standard deviation, and coefficient of variation of reservoir inflows for the historical and generated time series

Month	Historical time series			Generated time series		
	Average ( $10^6 \text{ m}^3$ )	Standard deviation ( $10^6 \text{ m}^3$ )	Coefficient of Variation	Average ( $10^6 \text{ m}^3$ )	Standard deviation ( $10^6 \text{ m}^3$ )	Coefficient of variation
October	25.2	11.1	0.44	26.6	9.9	0.37
November	32.2	14.5	0.45	33.7	12.8	0.37
December	59.7	41.1	0.69	60.8	38.4	0.63
January	83.4	81.9	0.98	86.9	73.8	0.85
February	108.1	74.8	0.69	110.7	68.8	0.62
March	143.2	83.5	0.58	146.7	74.4	0.51
April	143.1	86.3	0.6	144.8	77.2	0.53
May	76.9	49	0.64	79	47.4	0.6
June	39.7	26.3	0.66	37.7	25.1	0.67
July	31.5	13.4	0.43	29	12.1	0.42
August	27.5	11.5	0.42	25.7	9.7	0.38
September	25.9	11.1	0.43	26.7	9.5	0.36

**Table 3** Results of the Chi-square goodness-of-fit test for the inflow and evaporation data for all months

Month	Evaporation			Inflow		
	Test value ( $10^6 \text{ m}^3$ )	Degrees of freedom	Table value at 5% error area	Test value ( $10^6 \text{ m}^3$ )	Degrees of freedom	Table value at 5% error area
October	52.45	49	66.34	56.29	44	60.48
November	49.61	42	58.12	52.33	41	56.94
December	50.8	50	67.51	49.94	43	59.3
January	45.64	49	66.34	41.31	40	55.76
February	55.04	44	60.48	46.02	41	56.94
March	42.12	50	67.51	62.11	50	67.51
April	58.93	48	65.17	56.04	45	61.66
May	43.92	43	59.3	46.32	48	65.17
June	54.88	48	65.17	42	45	61.66
July	56.89	46	62.83	54.1	43	59.3
August	51.68	49	66.34	46.69	51	68.67
September	57.81	48	65.17	31.92	39	54.57

release was caused by the uncertainty of evaporation in September, while the lowest uncertainty occurred in May. The difference between the uncertainties in the months of April and May can be attributed to a failure in April. In April, the higher inflow to the reservoir and the lower water demand resulted in greater evaporation due to the larger storage and water surface area, which led to more uncertainty (higher standard

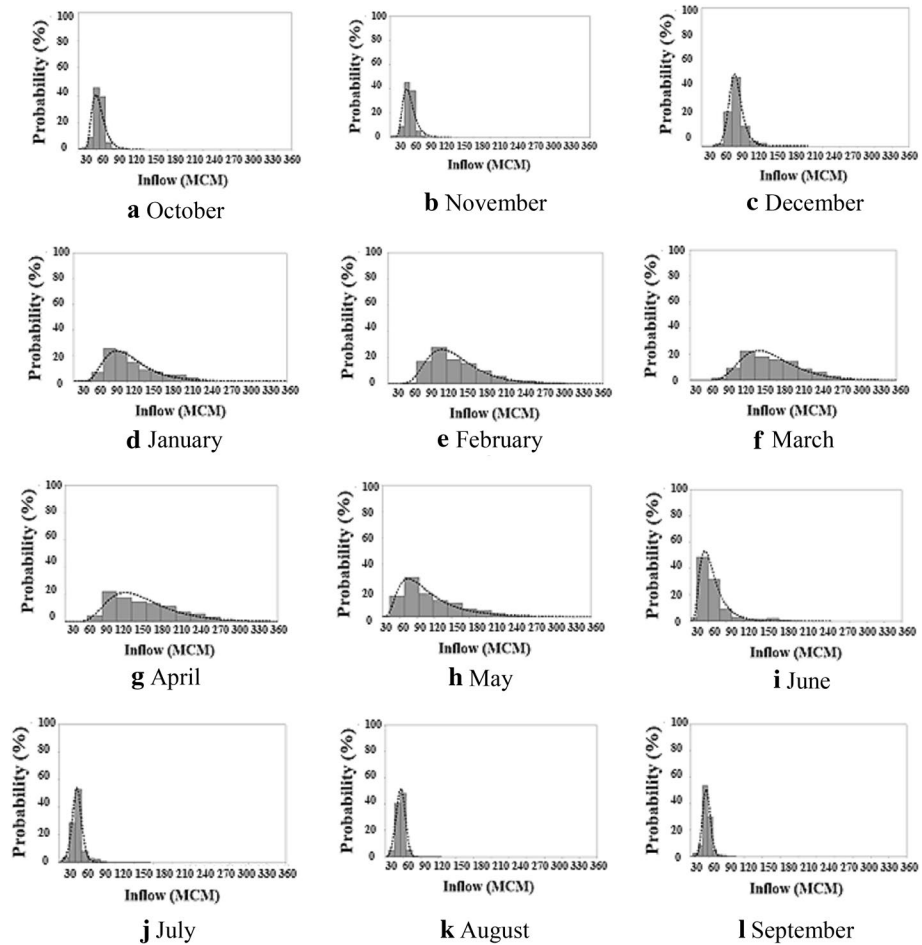


**Fig. 5** Distributions of the reservoir inflows in different months with the fitted lognormal distributions

deviation) in April than May. In the months of July and September, as the uncertainty of the evaporation variable was high, the uncertainty of water release increased. It should be noted that for the months that are not listed in Table 4, their release values are equal to the water demand values. Figure 7 shows the histograms of the reservoir releases in October, April, May, and September under the influence of the evaporation uncertainty. The least dispersion and uncertainty were observed in April. In contrast, the histogram of September exhibited the most dispersion, and the frequency distribution of the water releases was affected by the higher uncertainty of evaporation.

(2) Effect of inflow uncertainty on reservoir release

Table 4 shows the mean and standard deviation values of the reservoir releases under the influence of inflow uncertainty. According to Table 4, May has the least uncertainty of release and July has the highest release uncertainty. In other months that are not included in the table, the release values are fixed (i.e., no uncertainty). In October and

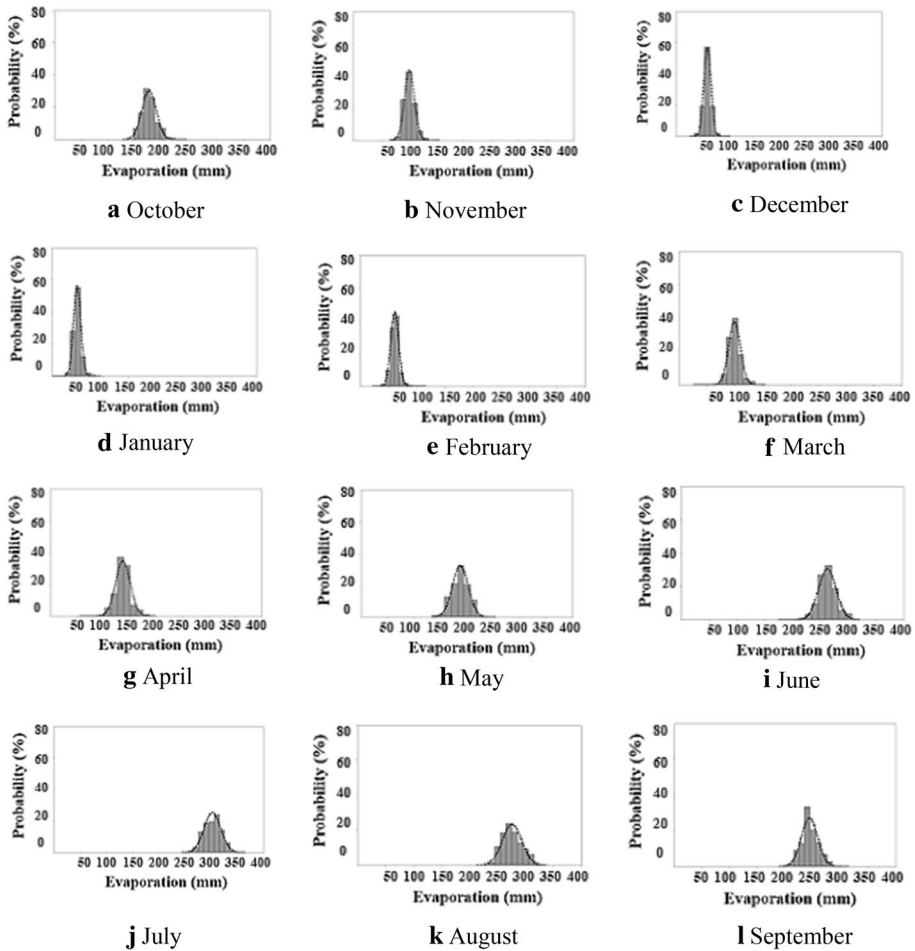


**Fig. 6** Distributions of the reservoir evaporation in different months with the fitted normal distributions

May of the lowest uncertainties, the release values are close to the water demands in most periods. That is, the number of the periods in which the reservoir failed to satisfy its downstream demands is limited. This can be attributed to the low water demand in October and the maximum storage of the reservoir in May, which also resulted in the successful operation of the reservoir in these two months. Thus, the output uncertainties for these two months are lower than those in other months. For the months from June to September with the higher water demands, their uncertainties are also higher. In these months, the number of failure periods is greater and hence the uncertainties in the water release are higher. The number of failures in July and the induced output uncertainties are higher than those in other months. Figure 8 shows the histograms of the reservoir water releases in the months of October, May, July, and September. The histograms indicate that July has the highest uncertainty, and May has the lowest uncertainty. The high-frequency values in October and May are close to the downstream water demands for the corresponding months.



**Table 4** Mean and standard deviation of reservoir release values in different months under the influences of the uncertainties of evaporation and inflow

Month	Water release influenced by evaporation		Water release influenced by inflow	
	Mean ( $10^6 \text{ m}^3$ )	Standard deviation ( $10^6 \text{ m}^3$ )	Mean ( $10^6 \text{ m}^3$ )	Standard deviation ( $10^6 \text{ m}^3$ )
October	16.5	0.05	18.98	0.97
April	113.2	0.11	–	–
May	139.31	0.04	148.34	0.87
June	106.54	0.13	119.57	3.92
July	72.54	0.15	81.35	4.49
August	81.43	0.13	85.41	3.92
September	60.42	0.15	64.1	2.8

(3) Effect of evaporation uncertainty on reservoir storage

Table 5 shows the mean and standard deviation values of the reservoir storage volumes resulting from the uncertainty of evaporation. According to Table 5, May and October, respectively, had the largest and smallest average storage volumes of the reservoir. In the months of October, November, and December, due to the lower inflows

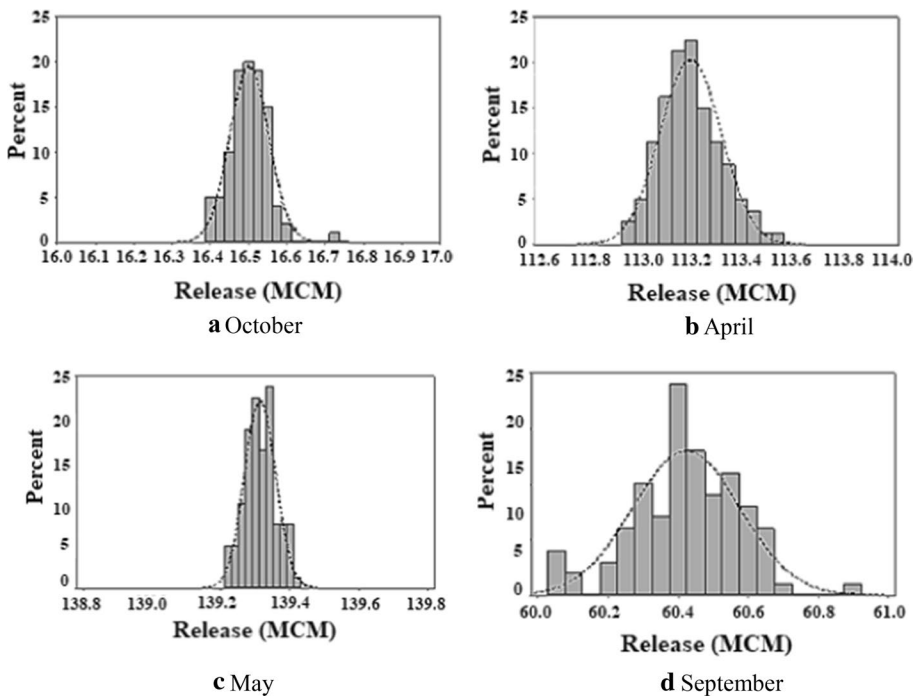


**Fig. 7** Histograms of reservoir releases influenced by the evaporation uncertainty for different months

of the reservoir, the storage was low and then gradually increased with the increase in the inflow into the reservoir. In May, the reservoir storage reached its maximum and then decreased with the increase in the output and the decrease in the input until September. The evaporation from the water surface of the reservoir was similar for different months. However, May had the smallest standard deviation of the storage volumes, while August and September showed the largest standard deviation values of the storage volumes. Because of the higher uncertainties of water release and evaporation, the months of August and September had the largest uncertainty of the reservoir storage. In May, because the average reservoir storage was at its highest level, the storage had the least uncertainty. Figure 9 shows the histograms of reservoir storage volumes under the influence of the uncertainty of evaporation for November, March, May, and August. It can be observed that the distributions of storage volumes in different months are closely related in terms of dispersion. But smaller and greater dispersions can be observed in May and August, respectively.

(4) Effect of inflow uncertainty on reservoir storage

Table 5 shows the mean and standard deviation values of the reservoir storage volumes under the influence of the inflow uncertainties in different months. Table 5 indicates that the reservoir storage was the lowest in October, gradually increased in the following months, reached the highest in May, and eventually decreased with the decreased inputs and increased releases from June to September. Depending on the uncertainty of the

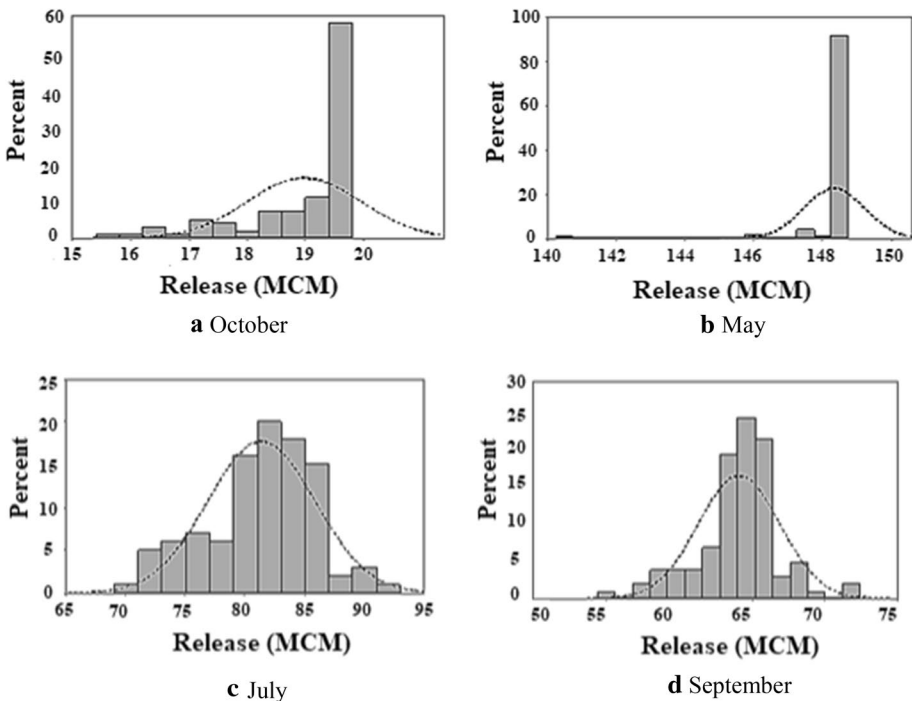


Fig. 8 Histograms of reservoir releases influenced by the inflow uncertainty for different months

inflows of the reservoir in different months, the storage volumes of the reservoir were also most uncertain in the months when the inflow uncertainties were higher. This is especially true for March, which had the highest uncertainty in the reservoir storage. The uncertainty of the reservoir inflow in April was greater than that of March. Also, the uncertainty of the storage in April was higher than that in March. It should be noted that in April, the number of periods in which the reservoir storage reached its highest level was greater than that in March, which led to the lower uncertainty in April. In October, the uncertainty of the storage volume of the reservoir was also the lowest. Due to the higher uncertainties of the inflows of the reservoir in August and September, the uncertainties of the storage volumes of the reservoir in these two months were lower than that in October. However, due to the lower uncertainty of the reservoir water release in October, the uncertainty of the reservoir storage in October was lower than those in August and September. Figure 10 shows the histograms of the reservoir storage volumes for October, March, May, and August under the influence of the uncertainty of the inflows into the reservoir. It can be found that the uncertainties of the reservoir storage volumes in May and March were greater than those in October and August.

In summary, in the months of August and September, there was a high uncertainty of water release and storage caused by the uncertainties of the reservoir evaporation and inflow. Note that the lowest inflow and the highest evaporation occurred in these two months. In contrast, May had the lowest uncertainties of reservoir storage and water release due to its highest storage level. Therefore, with the increase in the reservoir inflow mainly induced by heavy rainfall and snowmelt, the uncertainty of water release and reservoir storage tended to be lower.

**Table 5** Mean and standard deviation of reservoir storage in different months under the influence of the uncertainties of evaporation and inflow

Month	Evaporation		Inflow	
	Mean ( $10^6 \text{ m}^3$ )	Standard deviation ( $10^6 \text{ m}^3$ )	Mean ( $10^6 \text{ m}^3$ )	Standard deviation ( $10^6 \text{ m}^3$ )
October	445.73	0.46	432.73	21.53
November	448.25	0.47	435.42	22
December	472.35	0.48	460.56	23.29
January	529.18	0.48	516.93	32.5
February	608.07	0.48	603.59	35.59
March	692	0.47	699.34	36.22
April	753.42	0.47	776.2	32.21
May	753.8	0.39	783.46	30.83
June	683.07	0.44	705.72	31.87
July	605.6	0.48	612.62	29.46
August	553.01	0.5	548.61	26.21
September	488.94	0.5	478.74	23.42

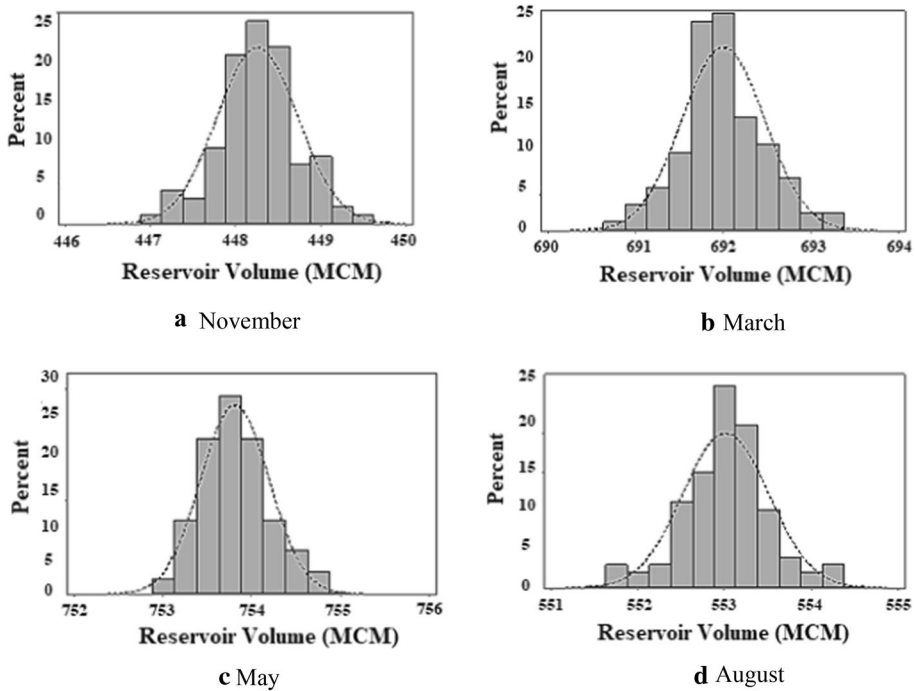


**Fig. 9** Histograms of reservoir storage volumes influenced by the evaporation uncertainty in different months

#### 4.5 Reservoir performance indices and uncertainty assessment

The three performance indices were used, in addition to the physical parameters of the reservoir, to evaluate the effects of the reservoir evaporation and inflow on the performances of the reservoir. For this purpose, the time-based and volumetric values of the reliability, resiliency, and vulnerability indices were calculated. It should be noted that higher reliability, lower vulnerability, and higher resiliency can make the reservoir operation more successful since higher reliability means higher water supply, lower vulnerability means a lower extent of failure, and higher resiliency implies a higher ability for the system to quickly recover from a failure. Note that the uncertainty of evaporation did not affect the time-based reliability and resiliency indices. In other words, the uncertainty of evaporation did not induce the change in the stage of the reservoir from failure to a successful state or vice versa. Also, the uncertainty of evaporation was not great enough to affect the uncertainty of resiliency. Table 6 lists the mean and standard deviation values of the volumetric reliability and vulnerability indices under the influence of evaporation uncertainty. According to Table 6, the magnitude of the failures in the vulnerability criterion was greater than the release volume changes in the volumetric reliability. Therefore, the uncertainty of vulnerability was higher than the uncertainty of the volumetric vulnerability. Figure 11 displays the histograms of the volumetric reliability and vulnerability indices under the influence of evaporation uncertainty. The histograms indicate that the vulnerability index exhibited greater dispersion than the volumetric reliability under the influence of

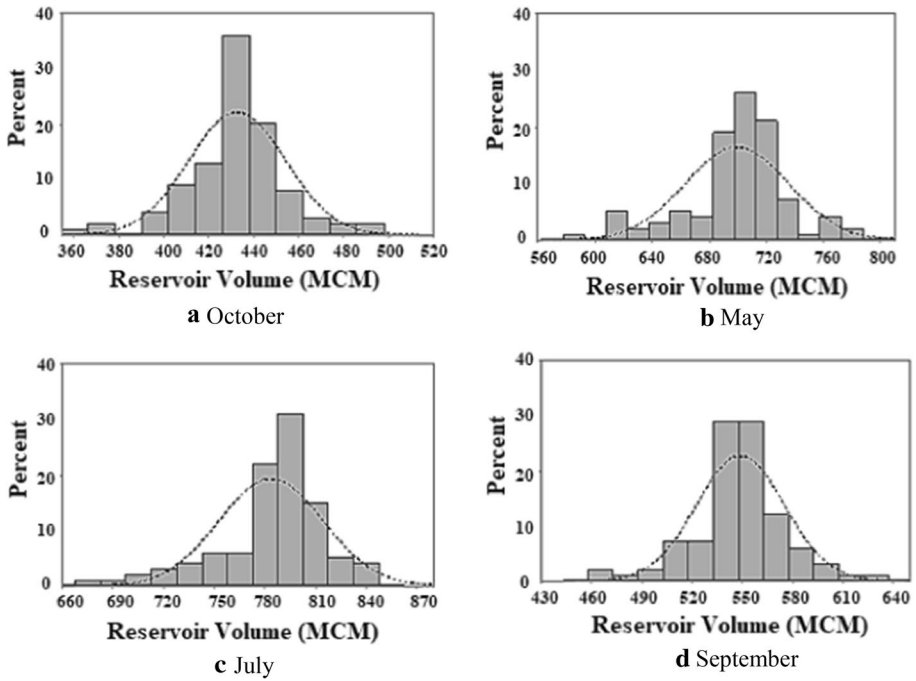


**Fig. 10** Histograms of reservoir storage volumes influenced by the inflow uncertainty in different months

the uncertainty of evaporation. Table 7 shows the details on the uncertainties of the three performance indices under the influence of the inflow uncertainty. Higher reliability values can be observed in Table 7 because when the inflows to the reservoir were high, the water demands were low and the reservoir operation was successful in most months of the year.

Considering the high values obtained for the reliability criterion, the reservoir seemed to be successful in meeting the water requirements. However, considering the obtained values for the resiliency and vulnerability criteria, it is obvious that this reservoir was not so successful. The operation of the reservoir resulted in low resiliency and high vulnerability values because in the standard operation policy the water supply demand was considered only in the current period. Failing to consider the supply demand in the following periods led to severe failures. It seems that adopting a better way to operate the reservoir (such as optimization) would reduce the level of vulnerability and increase resiliency. According to Table 7, the highest and lowest values of the coefficient of variation are related to the resiliency and the volumetric reliability, respectively. The histograms in Fig. 12 show the distributions of the performance indices under the influence of inflow uncertainty, indicating that the vulnerability has more dispersion than other indices and the least dispersion is related to the volumetric reliability.

**Table 6** Mean and standard deviation of volumetric reliability and vulnerability under the influence of the uncertainty of evaporation

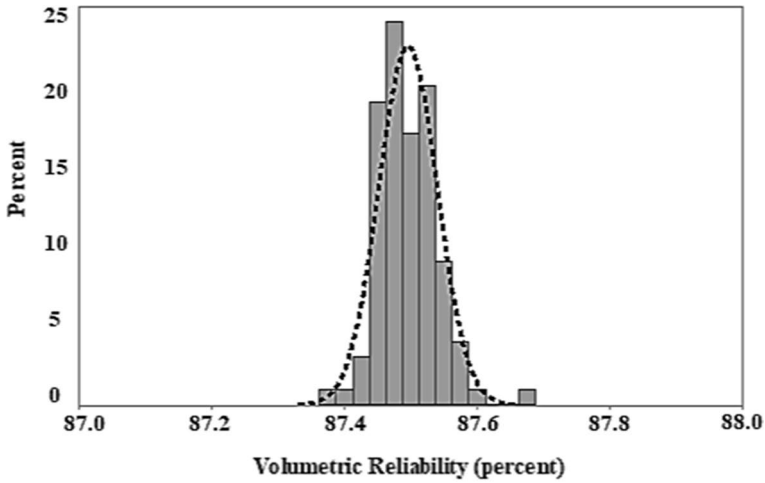
Performance index	Mean (%)	Standard deviation (%)
Volumetric Reliability	87.50	0.05
Vulnerability	80.02	0.50

## 5 Conclusion

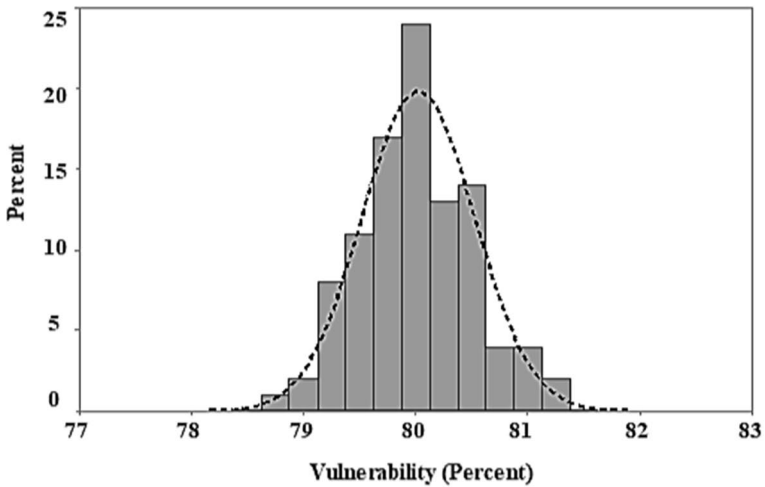
Uncertainty analysis of reservoir inflow and evaporation is crucial for efficient reservoir operation in order to decide the optimal water release for various purposes. For the variables that do not have 100% correlation, a joint uncertainty analysis should be implemented because a single uncertainty analysis has low accuracy. In other words, the lower correlation, the lower accuracy for a single uncertainty analysis. Due to the decrease in the annual inflow of Durudzan reservoir and the increase in its evaporation induced by the droughts in recent years, its water release has been reduced, which caused extensive socioeconomic damages. Therefore, uncertainty assessment of these variables is inevitable. In this study, the effects of the joint uncertainties of the evaporation and inflow of this reservoir on its performance variables (storage and release) were investigated. For this purpose, 100 time series of 47-year reservoir evaporation and inflow data were generated by using the Monte Carlo simulation and utilized to operate the reservoir using an artificial neural network and following the standard operation policy method.

The results showed that the lowest and highest reservoir inflows occurred in the driest months (September and October) and the wettest months (March and April), respectively, and hence April and September had the highest and lowest inflow uncertainties, respectively. Also, for the reservoir evaporation, July and January had the highest and lowest evaporation values, which resulted in the highest and lowest uncertainties of evaporation, respectively. Regarding the reservoir release and storage, the highest and lowest uncertainties of the reservoir release occurred, respectively, in July and May with standard deviation values of 4.49 and 0.87 (MCM) under the influence of the inflow uncertainty and, respectively, in September and May with standard deviation values of 0.15 and 0.04 (MCM) under the influence of the evaporation uncertainty. Therefore, May had the lowest uncertainty in water release under the influences of inflow and evaporation. The highest and lowest uncertainties of the reservoir storage occurred, respectively, in August and September and in May with standard deviation values of 0.50, 0.50, and 0.39 (MCM) under the influence of the evaporation uncertainty and, respectively, in March and October with standard deviation values of 36.22 and 21.53 (MCM) under the influence of the inflow uncertainty. It can be concluded that in months of July to September, there were higher uncertainties in both water release and storage of the reservoir under the influence of its inflow and evaporation.

According to the coefficient of variation, the highest uncertainty was related to the resiliency and the lowest uncertainty was associated with the volumetric reliability. Considering the values obtained for vulnerability and resiliency indices, it is recommended that reservoir operation policies with lower vulnerability and higher resiliency be adopted. Also, it is recommended that the uncertainties associated with the model and water demands be considered in future studies.



**a** Volumetric Reliability



**b** Vulnerability

**Fig. 11** Distributions of volumetric reliability and vulnerability indices under the influence of the evaporation uncertainty

**Table 7** Uncertainty assessment of performance indices under the influence of inflow uncertainty

Performance index	Mean (%)	Standard deviation (%)	Coefficient of variation
Time-based Reliability	92.13	92.13	0.024
Volumetric Reliability	93.11	93.11	0.020
Vulnerability	76.27	76.27	0.073
Resiliency	32.20	32.20	0.158

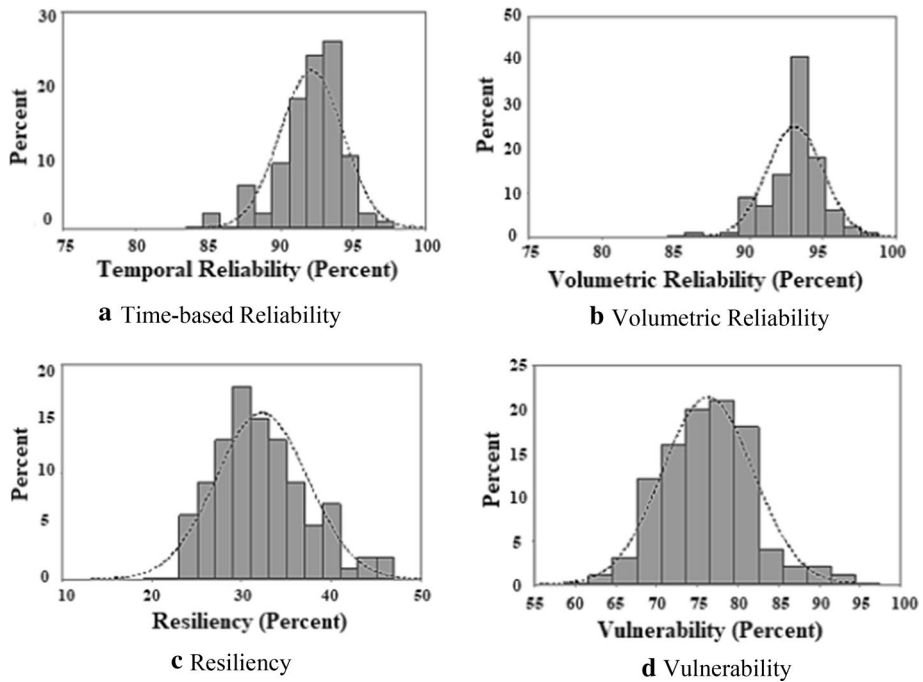


**Fig. 12** Distributions of performance indices under the influence of the inflow uncertainty

**Acknowledgements** The authors thank Iran's National Science Foundation (INSF) for the support for this research.

**Data Availability Statement** All of the required data have been presented in our article.

**Declarations**

**Conflict of interest** The authors declared that they have no conflict of interest.

## References

- Akbari-Alashti, H., Bozorg-Haddad, O., Fallah-Mehdipour, E., & Mariño, M. A. (2014). Multi-reservoir real-time operation rules: A new genetic programming approach. *Proceedings of the Institution of Civil Engineers: Water Management*, 167(10), 561–576. <https://doi.org/10.1680/wama.13.00021>
- Araghinejad, S. (2013). *Data-driven modeling: Using MATLAB® in water resources and environmental engineering*. Springer Science and Business Media.
- Asgari, H.-R., Bozorg-Haddad, O., Pazoki, M., & Loáiciga, H. A. (2016). Weed optimization algorithm for optimal reservoir operation. *Journal of Irrigation and Drainage Engineering*, 142(2), 04015055. [https://doi.org/10.1061/\(ASCE\)IR.1943-4774.0000963](https://doi.org/10.1061/(ASCE)IR.1943-4774.0000963)
- Ashofteh, P.-S., Bozorg-Haddad, O., & Loáiciga, H. A. (2019). Application of bi-objective genetic programming for optimizing irrigation rules using two reservoir performance criteria. *International Journal of River Basin Management*. <https://doi.org/10.1080/15715124.2019.1613415> in Press.
- Bai, Y., and Jin, W.-L. (2016). Random variables and uncertainty analysis. *Marine Structural Design*, 615–625.




- Bozorg-Haddad, O., (2018). "Water Resources Systems Optimization." Tehran university Publication, No.3, Tehran, Iran.
- Bozorg-Haddad, O., Athari, E., Fallah-Mehdipour, E., Bahrami, M., & Loáiciga, H. A. (2019). Allocation of reservoir releases under drought conditions: A conflict-resolution approach. *Proceedings of the Institution of Civil Engineers: Water Management*, 172(5), 218–228.
- Bozorg-Haddad, O., Azad, M., Fallah-Mehdipour, E., Delpasand, M., & Chu, X. (2020). Verification of FPA and PSO algorithms for rule curve extraction and optimization of single- and multi-reservoir systems' operations considering their specific purposes. *Water Supply*. <https://doi.org/10.2166/ws.2020.274>
- Bozorg-Haddad, O., Farhangi, M., Fallah-Mehdipour, E., & Mariño, M. A. (2014). Effects of inflow uncertainty on the performance of multireservoir systems. *Journal of Irrigation and Drainage Engineering*, 140(11), 04014035.
- Bozorg-Haddad, O., Moradi-Jalal, M., Mirmomeni, M., Kholghi, M. K. H., & Mariño, M. A. (2009). Optimal cultivation rules in multi-crop irrigation areas. *Irrigation and Drainage*, 58(1), 38–49. <https://doi.org/10.1002/ird.381>
- Bozorg-Haddad, O., Zarezadeh-Mehrizi, M., Abdi-Dehkordi, M., Loáiciga, H. A., & Mariño, M. A. (2016). A self-tuning ANN model for simulation and forecasting of surface flows. *Water Resources Management*, 30(9), 2907–2929. <https://doi.org/10.1007/s11269-016-1301-2>
- Chang, L. C., & Chang, F. J. (2009). Multi-objective evolutionary algorithm for operating parallel reservoir system. *Journal of Hydrology*, 377(1–2), 12–20.
- Cigizoglu, H. K. (2008). Artificial neural networks in water resources. In H. G. Coskun, H. K. Cigizoglu, & M. D. Maktav (Eds.), *NATO Science for peace and security series C: Environmental security* (pp. 115–148). Springer. [https://doi.org/10.1007/978-1-4020-6575-0\\_8](https://doi.org/10.1007/978-1-4020-6575-0_8)
- Cremon, M. A., Christie, M. A., and Gerritsen, M. G. (2018). "Monte Carlo Simulation for Uncertainty Quantification in Reservoir Simulation: A Convergence Study. In: Conference proceedings, ECMOR XVI - 16th european conference on the mathematics of oil, pp.1 - 18.
- Delli Priscoli, J. (2000). Water and civilization: Using history to reframe water policy debates and to build a new ecological realism. *Water Policy*, 1(6), 623–636. [https://doi.org/10.1016/s1366-7017\(99\)00019-7](https://doi.org/10.1016/s1366-7017(99)00019-7)
- Delpasand, M., Bozorg-Haddad, O., & Loáiciga, H. A. (2020). Integrated virtual water trade management considering self-sufficient production of strategic agricultural and industrial products. *Science of the Total Environment*. <https://doi.org/10.1016/j.scitotenv.2020.140797>
- Delpasand, M., Fallah-Mehdipour, E., Azizipour, M., Jalali, M., Safavi, H. R., Saghaian, B., Loáiciga, H. A., Babel, M. S., Savic, D., & Bozorg-Haddad, O. (2021). Forensic engineering analysis applied to flood control. *Journal of Hydrology*, 594, 125961.
- Du, Y.-C., & Stephanus, A. (2018). Levenberg-Marquardt neural network algorithm for degree of arteriovenous fistula stenosis classification using a dual optical photoplethysmography sensor. *Sensors*, 18(7), 2322. <https://doi.org/10.3390/s18072322>
- Duckstein, L., & Plate, E. J. (Eds.). (1987). *Engineering reliability and risk in water resources*. Springer. <https://doi.org/10.1007/978-94-009-3577-8>
- Ehsani, N., Fekete, B. M., Vörösmarty, C. J., & Tessler, Z. D. (2015). A neural network based general reservoir operation scheme. *Stochastic Environmental Research and Risk Assessment*, 30(4), 1151–1166. <https://doi.org/10.1007/s00477-015-1147-9>
- Fallah-Mehdipour, E., Bozorg-Haddad, O., & Mariño, M. A. (2015). Evaluation of stakeholder utility risk caused by the objective functions in multipurpose multireservoir systems. *Journal of Irrigation and Drainage Engineering*, 141(2), 04014047. [https://doi.org/10.1061/\(ASCE\)IR.1943-4774.0000785](https://doi.org/10.1061/(ASCE)IR.1943-4774.0000785)
- González-Manteiga, W., & Crujeiras, R. M. (2013). An updated review of goodness-of-fit tests for regression models. *TEST*, 22(3), 361–411. <https://doi.org/10.1007/s11749-013-0327-5>
- Hashimoto, T., Stedinger, J. R., & Loucks, D. P. (1982). Reliability, resiliency, and vulnerability criteria for water resource system performance evaluation. *Water Resources Research*, 18(1), 14–20.
- Iyer, M. S., & Rhinehart, R. R. (1999). A method to determine the required number of neural-network training repetitions. *IEEE Transactions on Neural Networks*, 10(2), 427–432. <https://doi.org/10.1109/72.750573>
- Jain, S. K., Das, A., & Srivastava, D. K. (1999). Application of ANN for reservoir inflow prediction and operation. *Journal of Water Resources Planning and Management*, 125(5), 263–271. [https://doi.org/10.1061/\(asce\)0733-9496\(1999\)125:5\(263\)](https://doi.org/10.1061/(asce)0733-9496(1999)125:5(263))
- Jain, S. K., Reddy, N. S. R. K., & Chaube, U. C. (2005). Analysis of a large inter-basin water transfer system in India. *Water and Energy Abstracts*, 15(2), 32–32.

- Jothivenkatachalam, K., Nithya, A., & Mohan, S. C. (2010). Correlation analysis of drinking water quality in and around perur block of Coimbatore District, Tamil Nadu, India. *Rasayan Journal of Chemistry*, 3(4), 649–654.
- Karamouz, M., and Araghinejad, Sh. (2011), “Advanced Hydrology”, Industrial university of Amir Kabir publication, No. 2, Tehran, Iran.
- King, L. M., & Simonovic, S. P. (2020). A deterministic Monte Carlo simulation framework for dam safety flow control assessment. *Water*, 12(2), 505.
- Lee, J., Lee, M., Chun, Y.-Y., & Lee, K. (2018). Uncertainty analysis of the water scarcity footprint based on the AWARE model considering temporal variations. *Water*, 10(3), 341. <https://doi.org/10.3390/w10030341>
- Liu, X., Lu, C., Zhu, Y., Singh, V. P., Qu, G., & Guo, X. (2017). Multi-objective reservoir operation during flood season considering spillway optimization. *Journal of Hydrology*, 552, 554–563.
- Loucks, D. P., Stedinger, J. R., & Haith, D. A. (1981). Water resource systems planning and analysis Prentice-Hall Englewood Cliffs NJ. *Hydrological Science*, 41(5), 697–713.
- Loucks, D. P., and van Beek, E. (2005). Water Resources Systems Planning and Management: An Introduction to Methods, Models and Applications. In: Studies and Reports in Hydrology. UNESCO Publishing, Paris.
- Lowe, L. D., Webb, J. A., Nathan, R. J., Etchells, T., & Malano, H. M. (2009). Evaporation from water supply reservoirs: An assessment of uncertainty. *Journal of Hydrology*, 376(1–2), 261–274.
- Maitly, R. (2018). Basic statistical properties of data. Springer transactions in civil and environmental engineering, 53–92. [https://doi.org/10.1007/978-981-10-8779-0\\_3](https://doi.org/10.1007/978-981-10-8779-0_3).
- Marton, D., & Paseka, S. (2017). Uncertainty impact on water management analysis of open water reservoir. *Environments*, 4(1), 10.
- McMillan, H., Seibert, J., Petersen-Overleir, A., Lang, M., White, P., Snelder, T., & Kiang, J. (2017). How uncertainty analysis of streamflow data can reduce costs and promote robust decisions in water management applications. *Water Resources Research*, 53(7), 5220–5228.
- Okon, A. N., Adewole, S. E., & Uguma, E. M. (2020). Artificial neural network model for reservoir petrophysical properties: Porosity, permeability and water saturation prediction. *Modeling Earth Systems and Environment*. <https://doi.org/10.1007/s40808-020-01012-4>
- Rolke, W., & Gongora, C. G. (2020). A chi-square goodness-of-fit test for continuous distributions against a known alternative. *Computational Statistics*. <https://doi.org/10.1007/s00180-020-00997-x>
- Seifollahi-Aghmiuni, S., Bozorg-Haddad, O., & Loáiciga, H. A. (2016). Development of a sample multi-tribute, multireservoir system for testing operational models. *Journal Irrigation and Drainage Engineering*, 142(1), 04015039.
- Shokri, A., Bozorg-Haddad, O., & Mariño, M. A. (2013). Algorithm for increasing the speed of evolutionary optimization and its accuracy in multi-objective problems. *Water Resources Management*, 27(7), 2231–2249. <https://doi.org/10.1007/s11269-013-0285-4>
- Soltanjilili, M., Bozorg-Haddad, O., & Mariño, M. A. (2011). Effect of breakage level one in design of water distribution networks. *Water Resources Management*, 25(1), 311–337. <https://doi.org/10.1007/s11269-010-9701-1>
- Soundharajan, B.-S., Adeloye, A. J., & Remesan, R. (2016). Evaluating the variability in surface water reservoir planning characteristics during climate change impacts assessment. *Journal of Hydrology*, 538, 625–639.
- Srdjevic, B., Medeiros, Y. D. P., & Faria, A. S. (2004). An objective multi-criteria evaluation of water management scenarios. *Water Resources Management*, 18(1), 35–54.
- Tegegne, G., & Kim, Y.-O. (2020). Representing inflow uncertainty for the development of monthly reservoir operations using genetic algorithms. *Journal of Hydrology*, 586, 124876.
- Tehrani, M., Samani, J., & Montaseri, M. (2008). Uncertainty analysis of reservoir sedimentation using latin hypercube sampling and Harr’s method: Shahar Chai Dam in Iran. *Journal of Hydrology (New Zealand)*, 47(1), 25–42.
- Willis, R., Finney, B. A., & Chu, W.-S. (1984). Monte Carlo optimization for reservoir operation. *Water Resources Research*, 20(9), 1177–1182.
- Xu, C.-Y., & Singh, V. P. (1998). A review on monthly water balance models for water resources investigations. *Water Resources Management*, 12(1), 20–50. <https://doi.org/10.1023/a:1007916816469>
- Zhang, X., Liang, F., Srinivasan, R., & Van Liew, M. (2009). Estimating uncertainty of streamflow simulation using Bayesian neural networks. *Water Resources Research*. <https://doi.org/10.1029/2008WR007030>
- Zhao, T., Cai, X., & Yang, D. (2011). Effect of streamflow forecast uncertainty on real-time reservoir operation. *Advances in Water Resources*, 34(4), 495–504.

**Publisher's Note** Springer Nature remains neutral with regard to jurisdictional claims in published maps and institutional affiliations.

## Authors and Affiliations

Omid Bozorg-Haddad<sup>1</sup>  · Pouria Yari<sup>1</sup> · Mohammad Delpasand<sup>2</sup> · Xuefeng Chu<sup>3</sup>

Pouria Yari  
Yari.Pouria@ut.ac.ir

Mohammad Delpasand  
Delpasand.m@ut.ac.ir

Xuefeng Chu  
Xuefeng.Chu@ndsu.edu

<sup>1</sup> Department of Irrigation & Reclamation Engineering, College of Agriculture & Natural Resources, University of Tehran, Karaj, Iran

<sup>2</sup> Department of Irrigation & Reclamation Engineering, Faculty of Agricultural Engineering & Technology, College of Agriculture & Natural Resources, University of Tehran, Karaj, Tehran, Iran

<sup>3</sup> Dept. of Civil & Environmental Engineering, North Dakota State Univ., Dept 2470, Fargo, ND 58108-6050, USA